

Figure 2.5-46 Low-Frequency, 10^{-5} Median, Magnitude-Distance Deaggregation Using Updated Source and Ground Motion Models

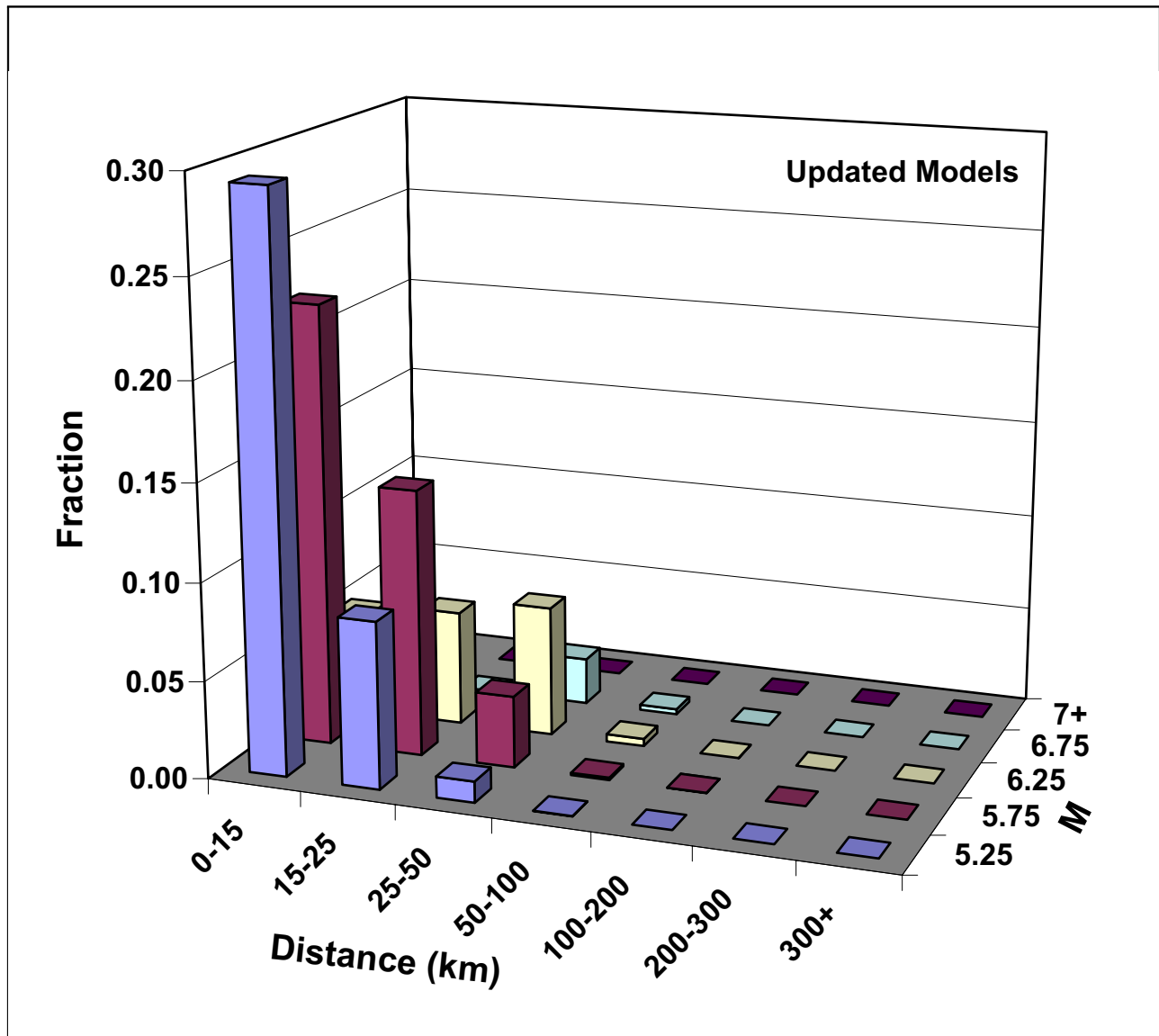


Figure 2.5-47 High-Frequency, 10^{-5} Median, Magnitude-Distance Deaggregation Using Updated Source and Ground Motion Models

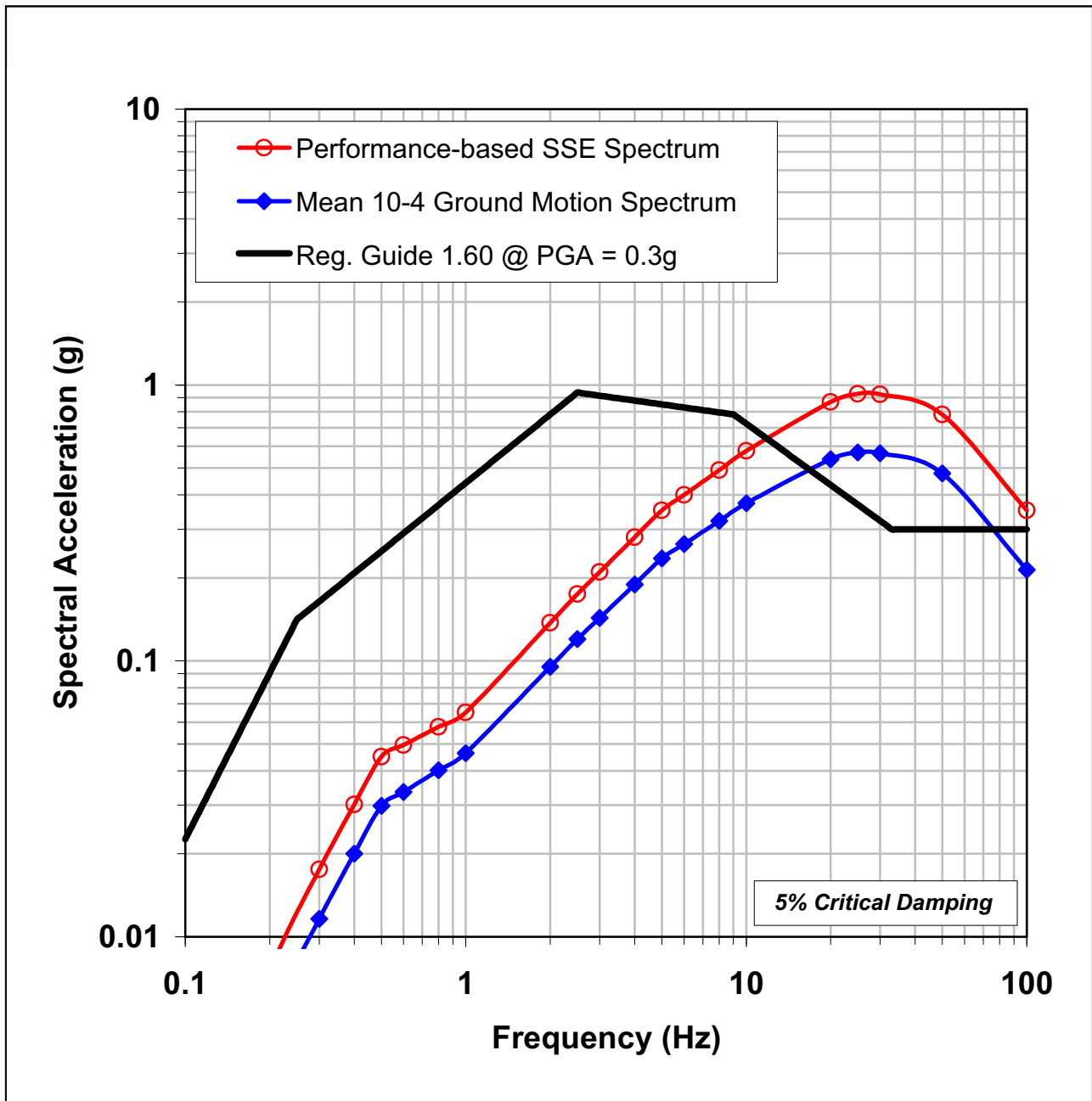


Figure 2.5-48 Selected Performance-Based Horizontal SSE Response Spectrum, As Scaled from Mean 10⁻⁴ Ground Motion Spectrum, Compared to RG 1.60 Spectrum Anchored to 0.3g

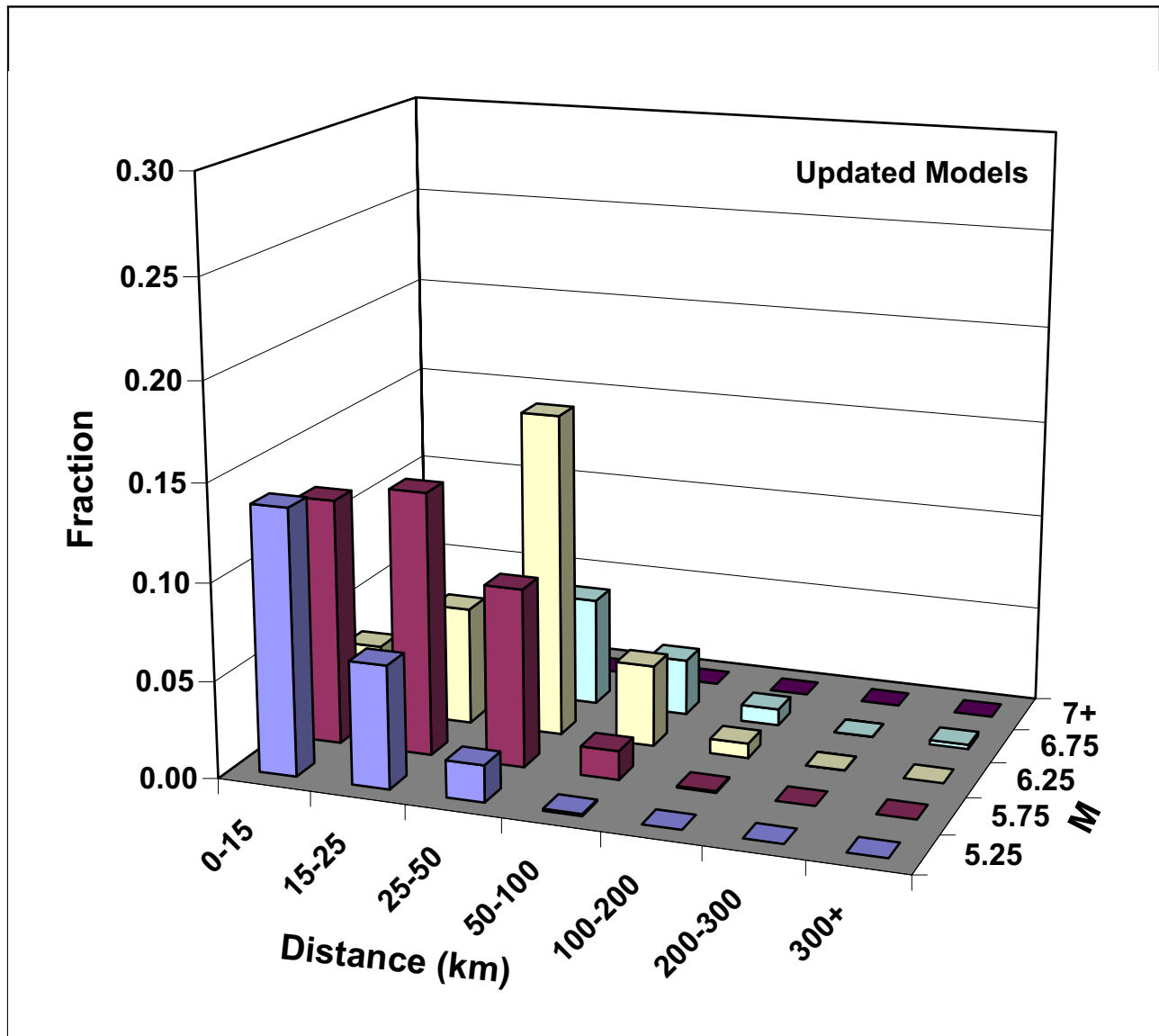


Figure 2.5-49 Magnitude-Distance Deaggregation for Low-Frequencies (1 and 2.5 Hz) at a Mean Annual Frequency of 5×10^{-5} Using Updated Source and Ground Motion Models

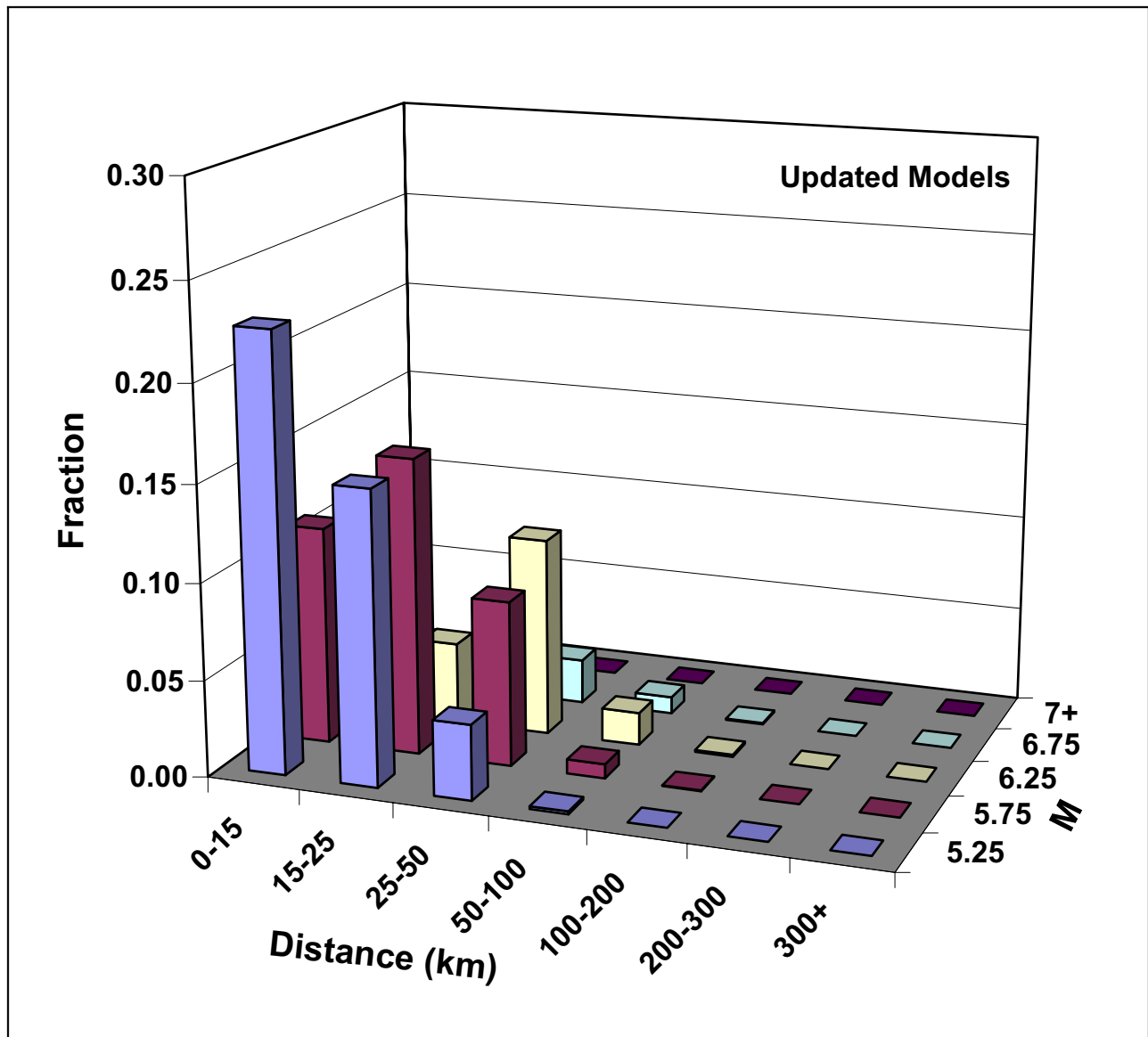


Figure 2.5-50 Magnitude-Distance Deaggregation for High-Frequencies (5 and 10 Hz) at a Mean Annual Frequency of 5×10^{-5} Using Updated Source and Ground Motion Models

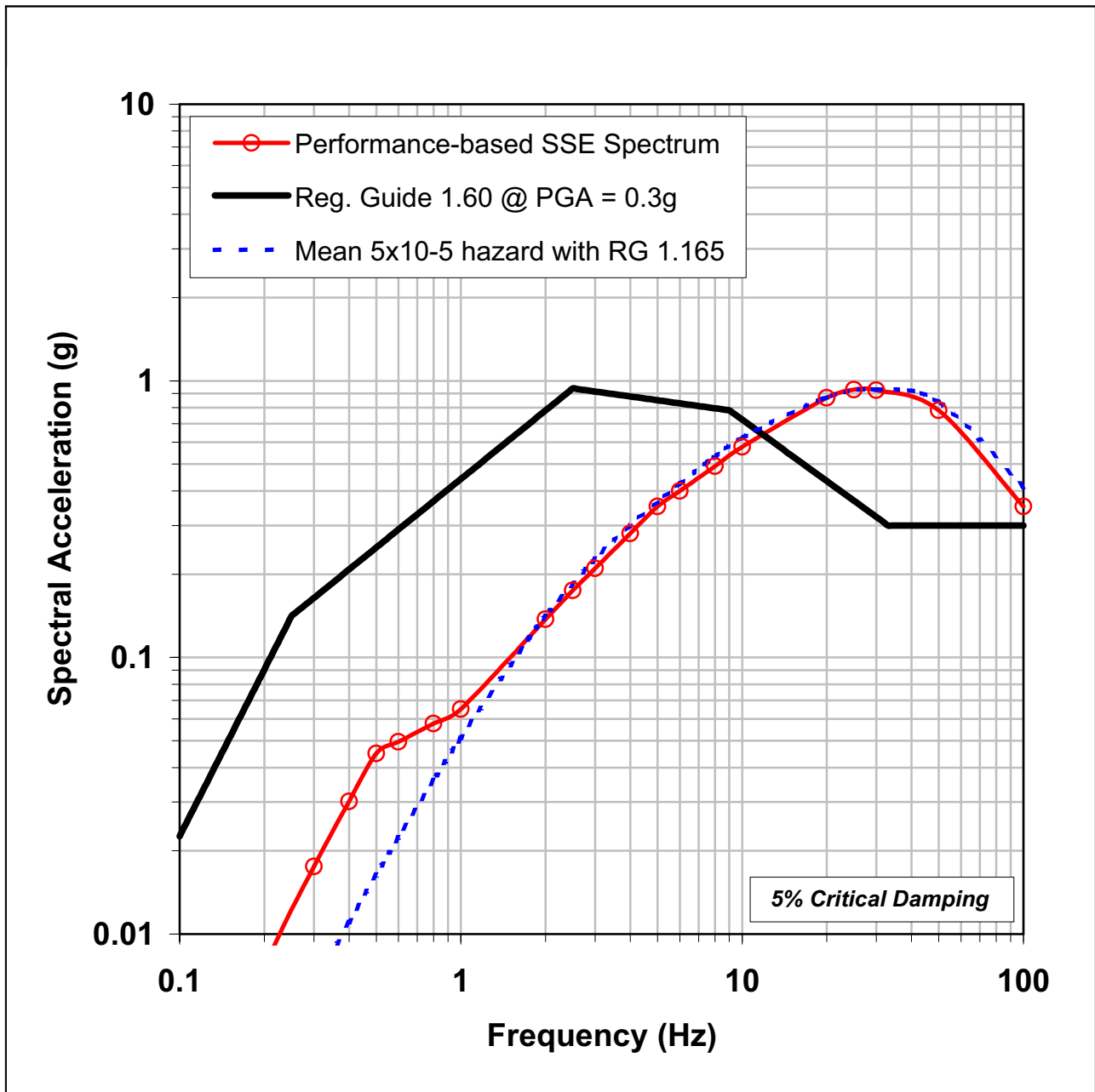


Figure 2.5-51 Horizontal Ground Motion Spectrum Calculated for Reference Probability of Mean 5×10^{-5} , Compared to RG 1.60 Spectrum Anchored to 0.3g and to Selected SSE Spectrum

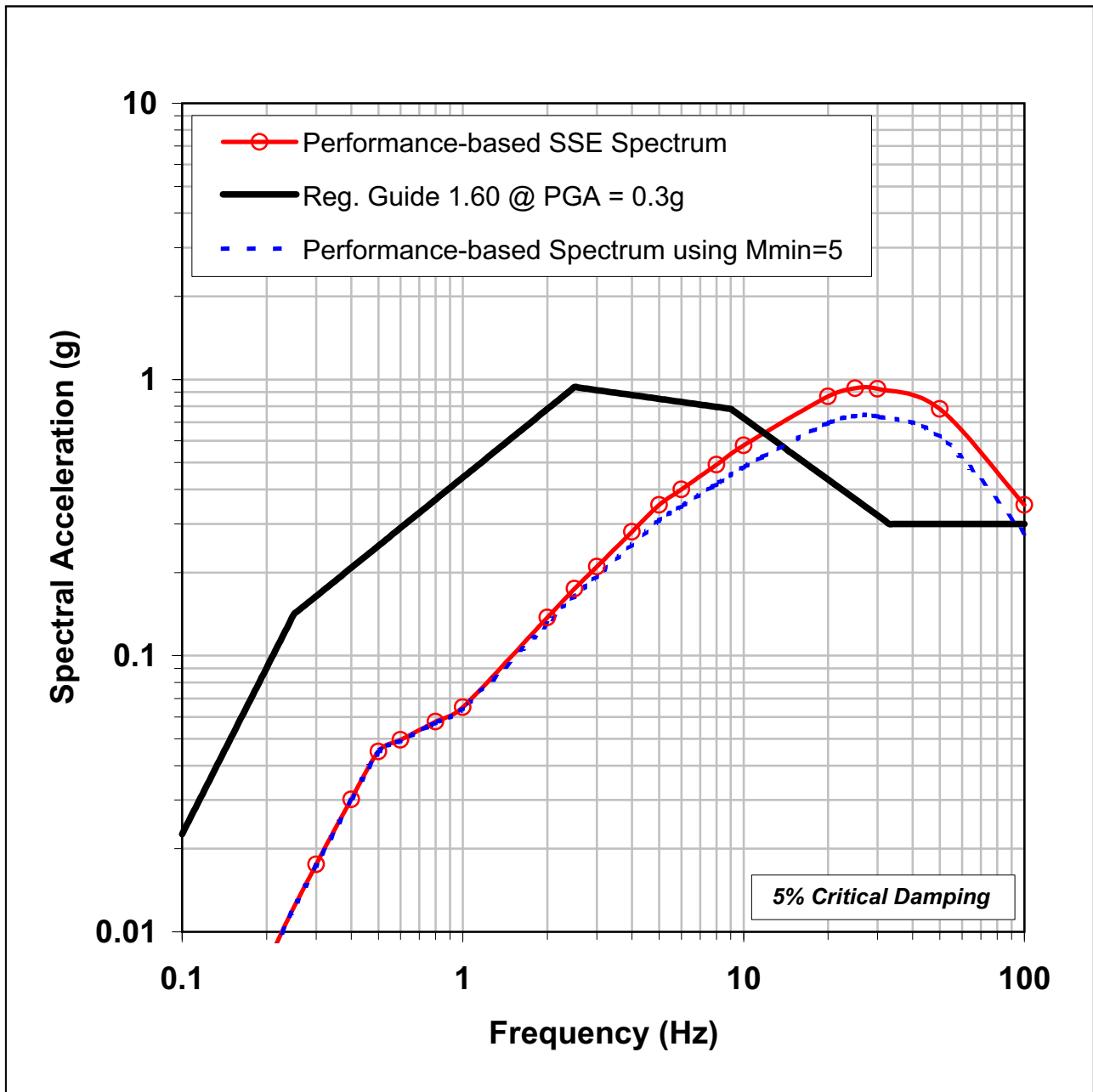


Figure 2.5-52 Sensitivity Plot of Scaled Spectrum Calculated Using Alternative Lower-Bound M of 5.0 and Scaling Factors in Table 2.5-27, Compared to RG 1.60 Spectrum Anchored to 0.3g and to Selected SSE Spectrum

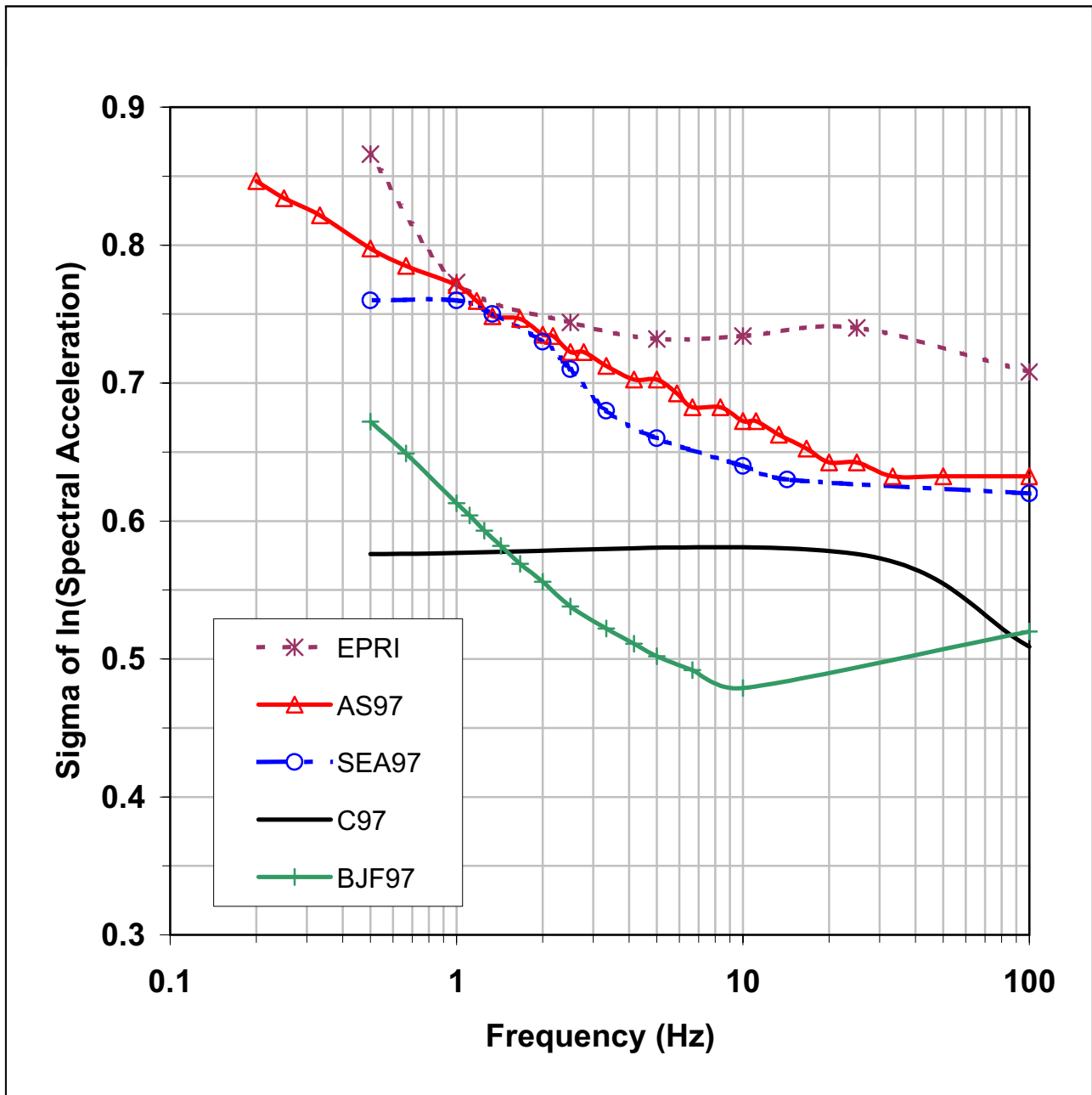


Figure 2.5-53 Comparison of Aleatory Sigmas Reported for California with Weighted Average Aleatory Sigma from EPRI Ground Motion 2003 Models for $M = 5.5$, $R_{CD} = 20$ km

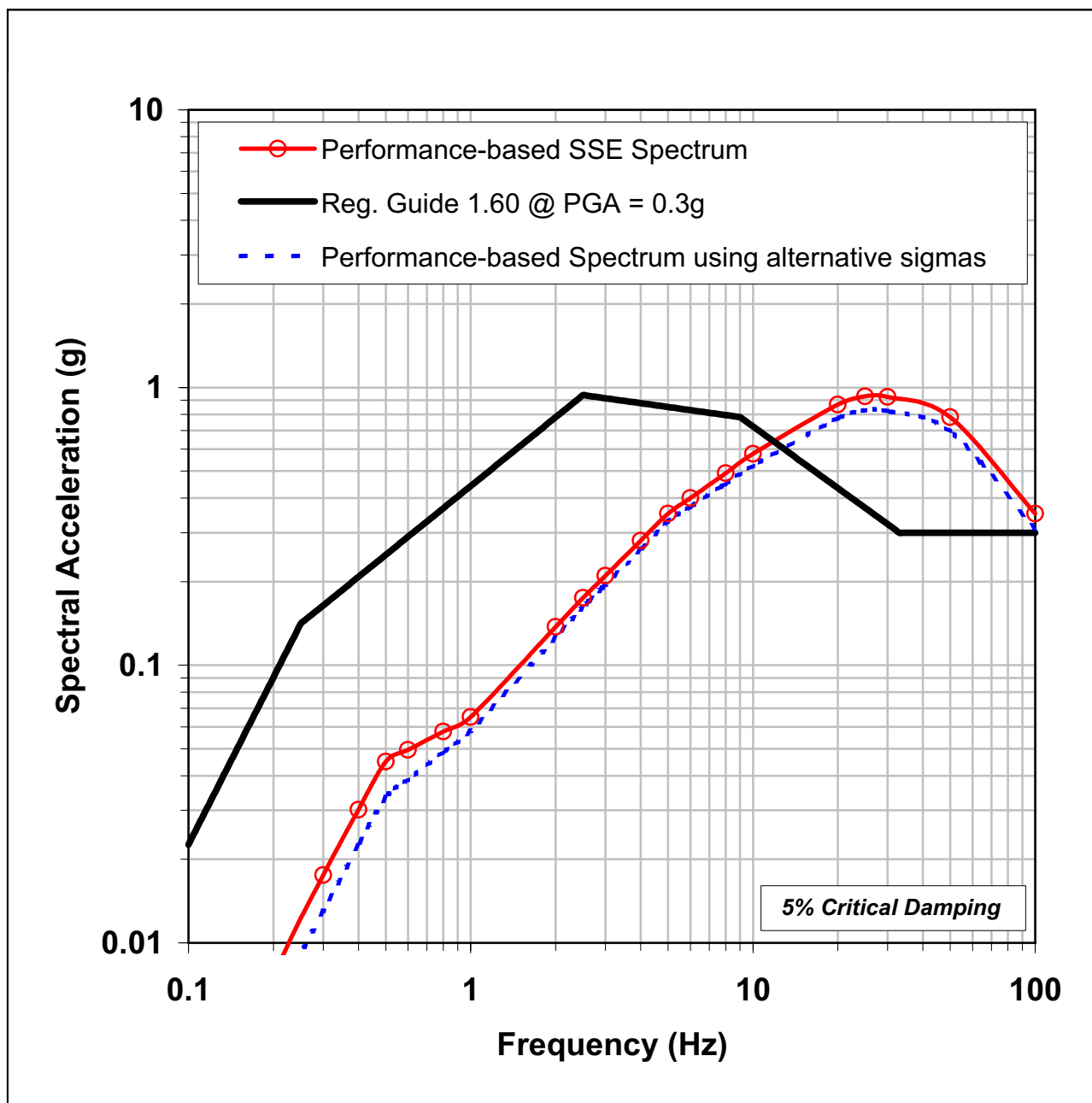


Figure 2.5-54 Sensitivity Plot of Scaled Spectrum Calculated Using Alternative Ground Motion Aleatory Uncertainties and Scaling Factors in Table 2.5-28, Compared to RG 1.60 Spectrum Anchored to 0.3g and to Selected SSE Spectrum

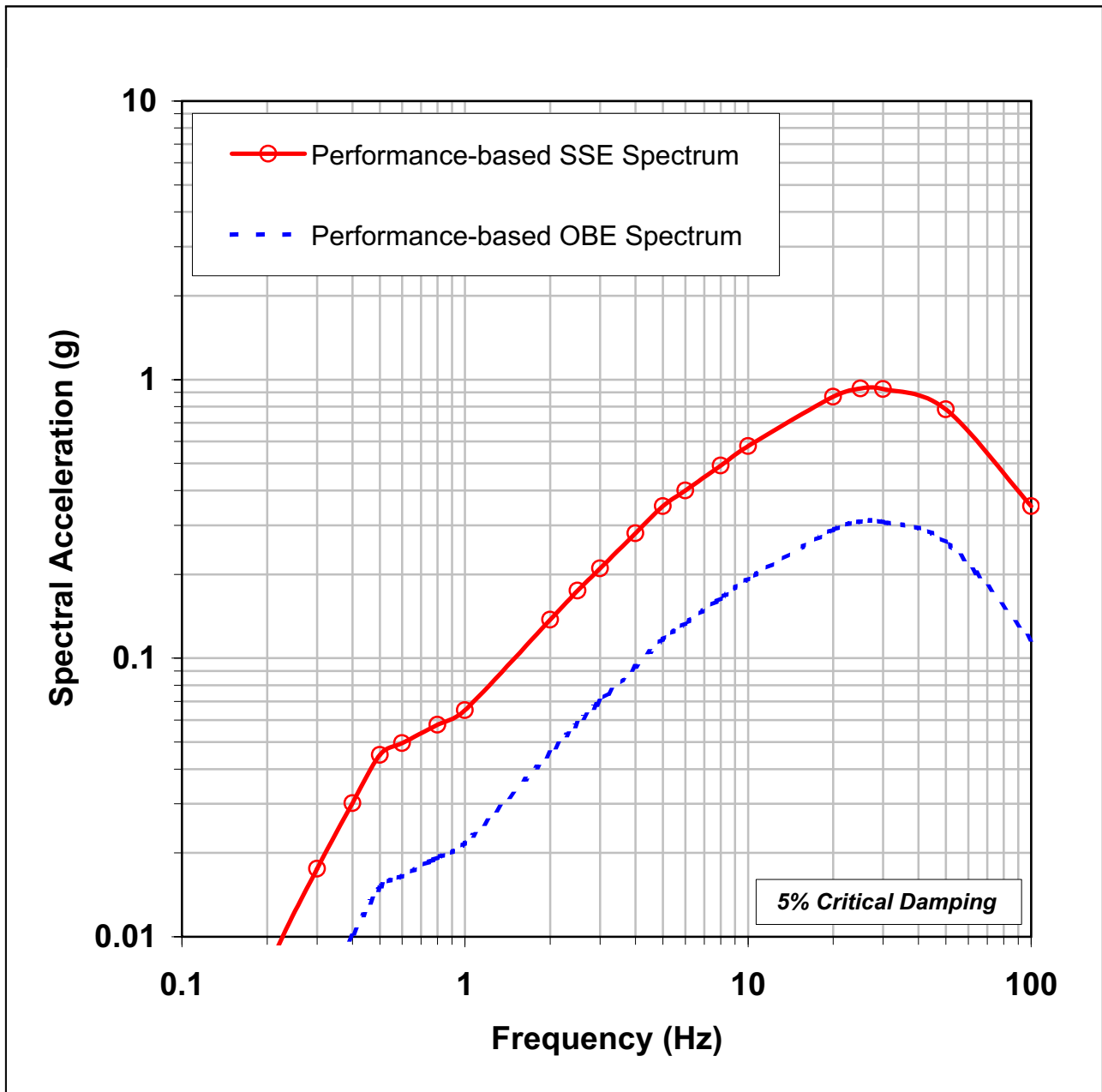


Figure 2.5-55 Horizontal SSE and OBE Response Spectra Based on Updated Models (5% of Critical Damping)

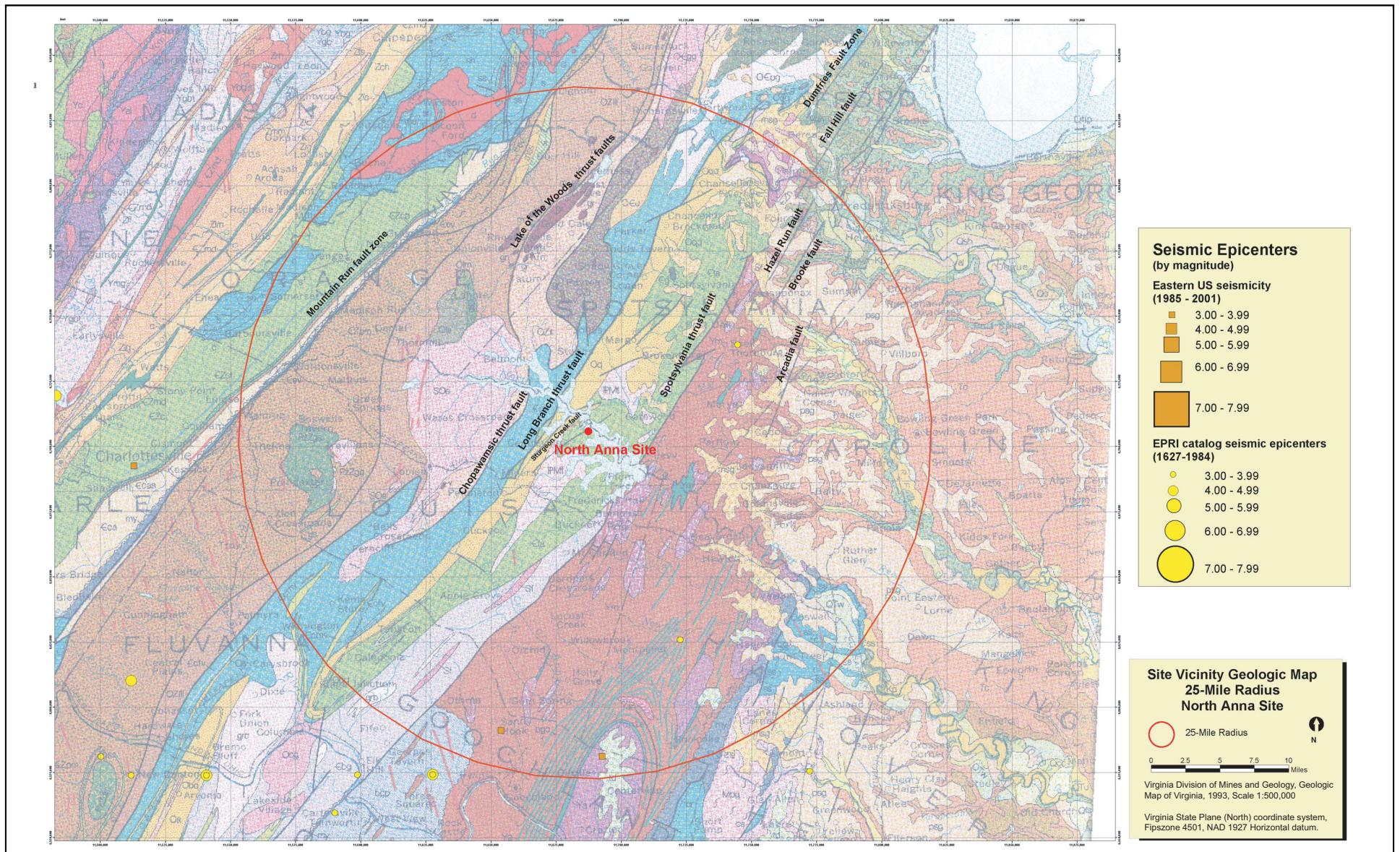


Figure 2.5-56 Site Vicinity Geologic Map and Seismicity (25-Mile Radius)

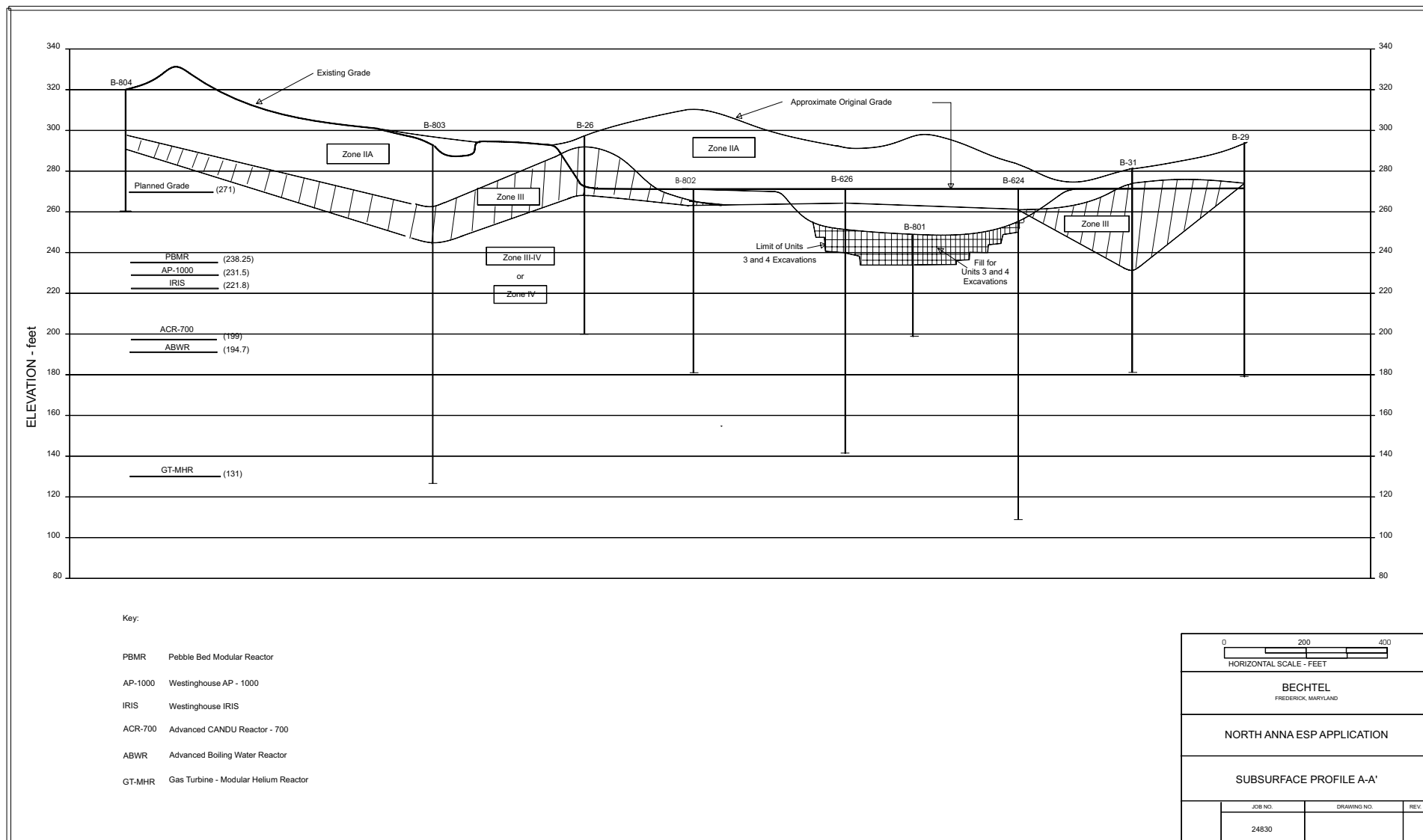


Figure 2.5-57 Subsurface Profile A-A'

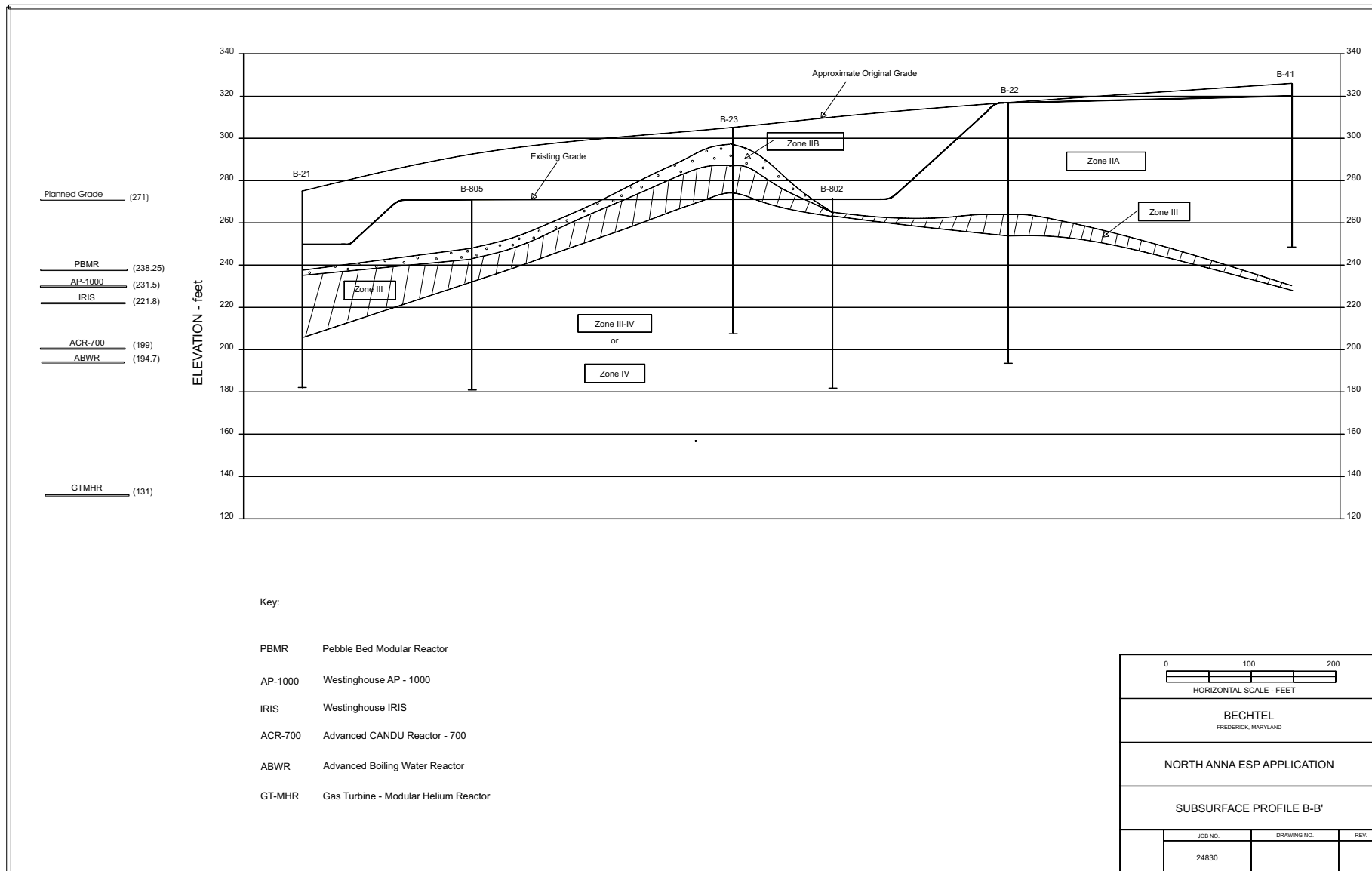


Figure 2.5-58 Subsurface Profile B-B'

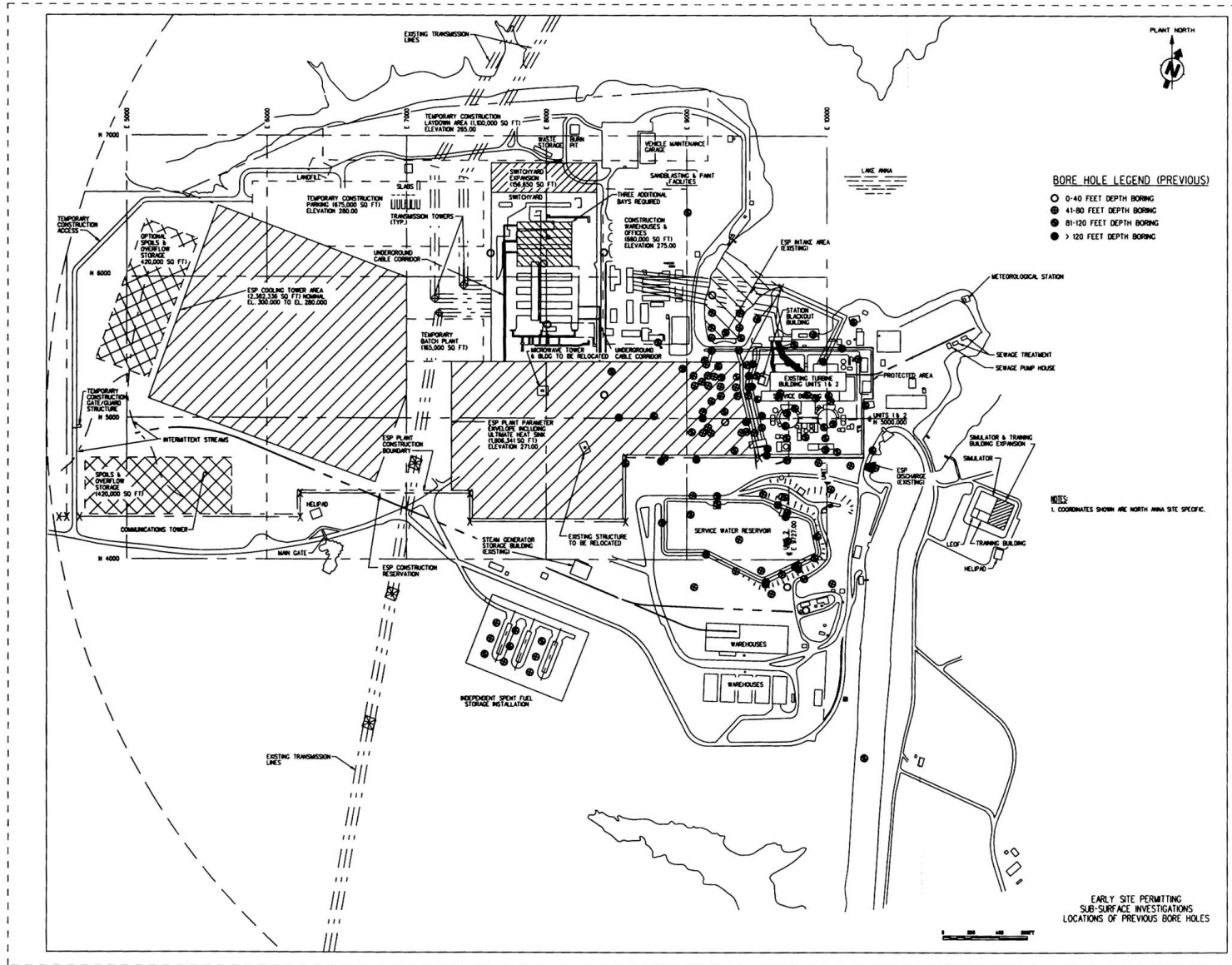


Figure 2.5-59 Locations of Previous Boreholes

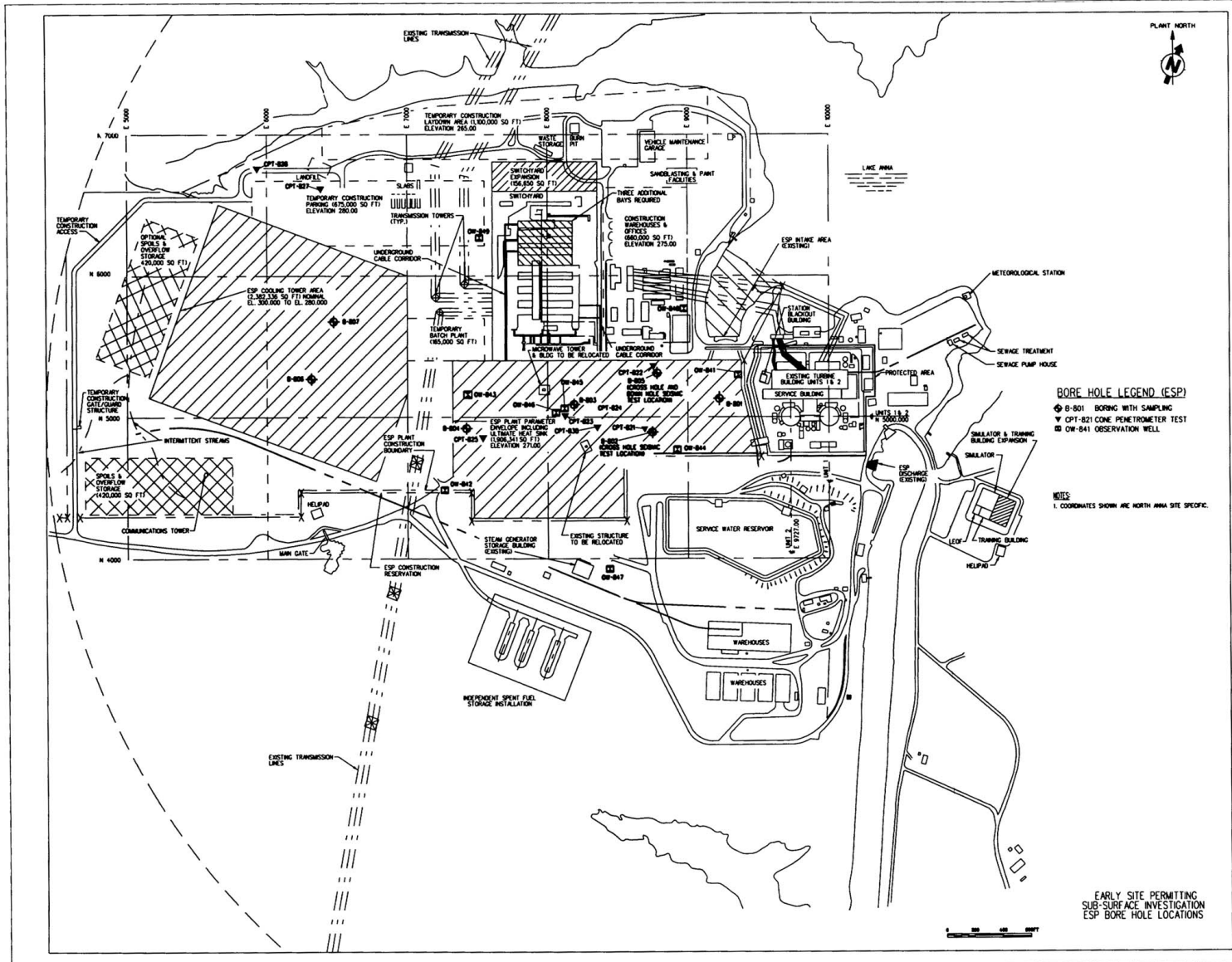


Figure 2.5-60 ESP Borehole Locations

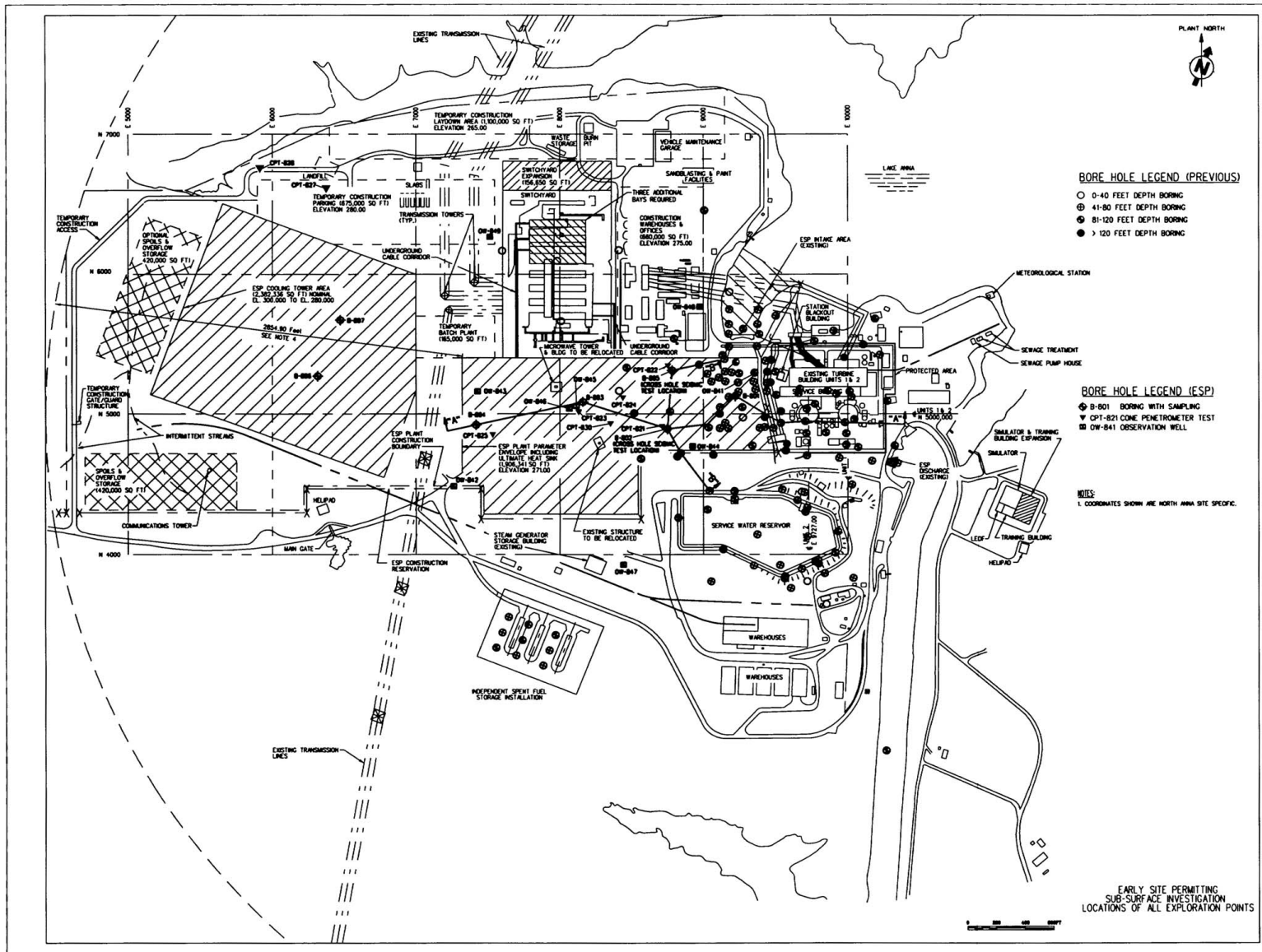


Figure 2.5-61 Locations of All Exploration Points

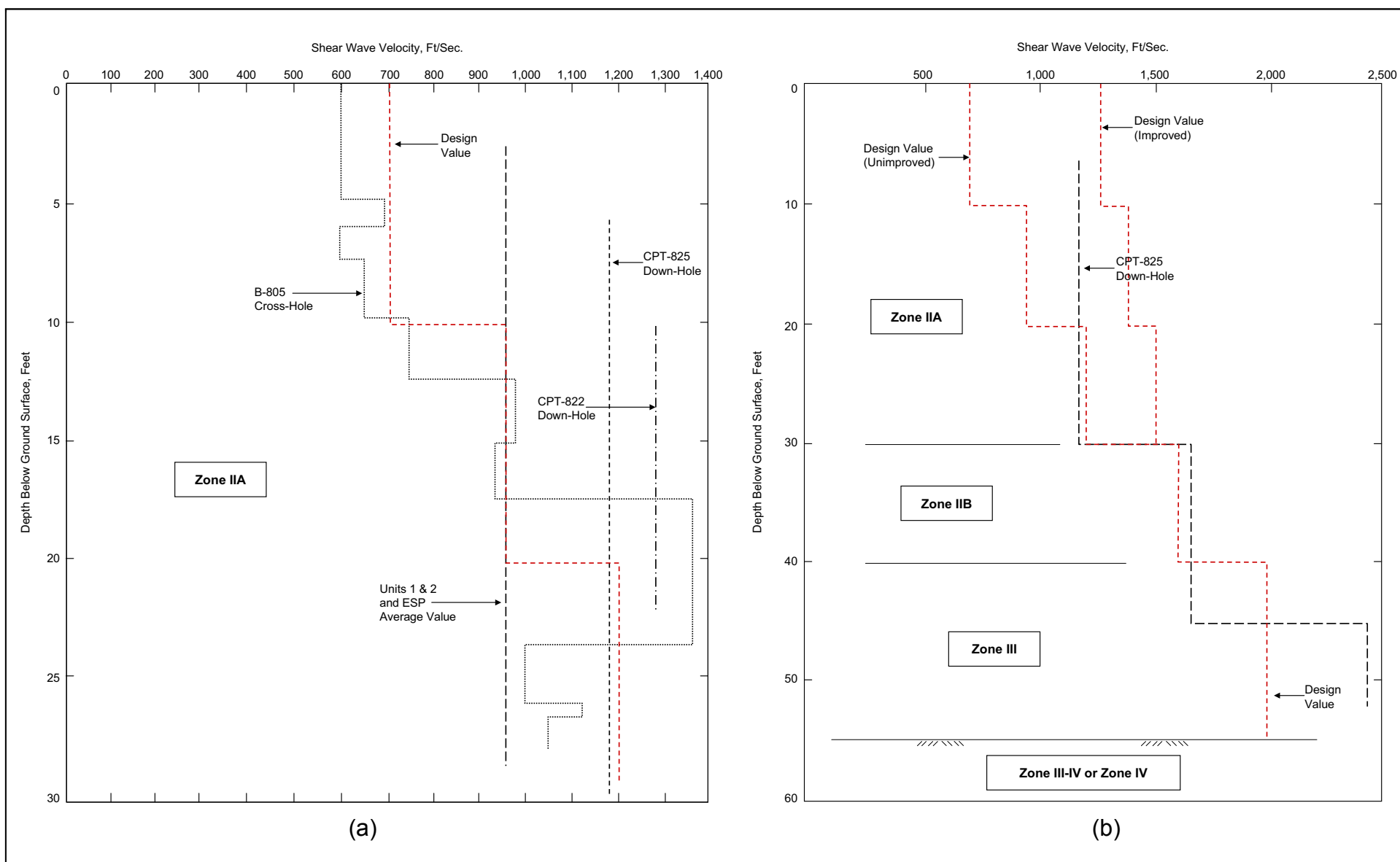


Figure 2.5-62 Zone IIA Shear Wave Velocity Profile (a) Full-Depth Shear Wave Velocity Profile (b)

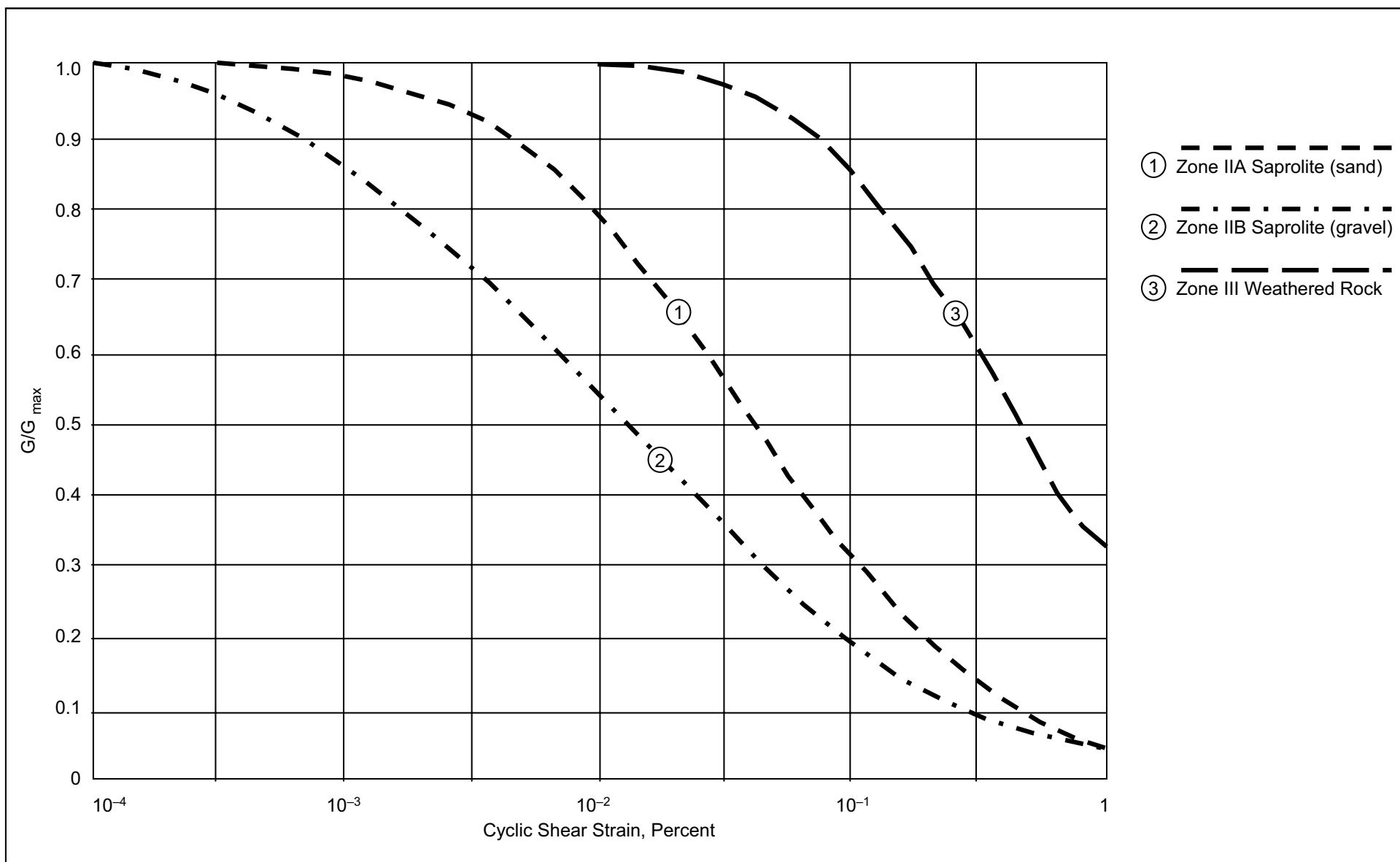


Figure 2.5-63 Variation of Normalized Shear Modulus with Cycle Shear Strain

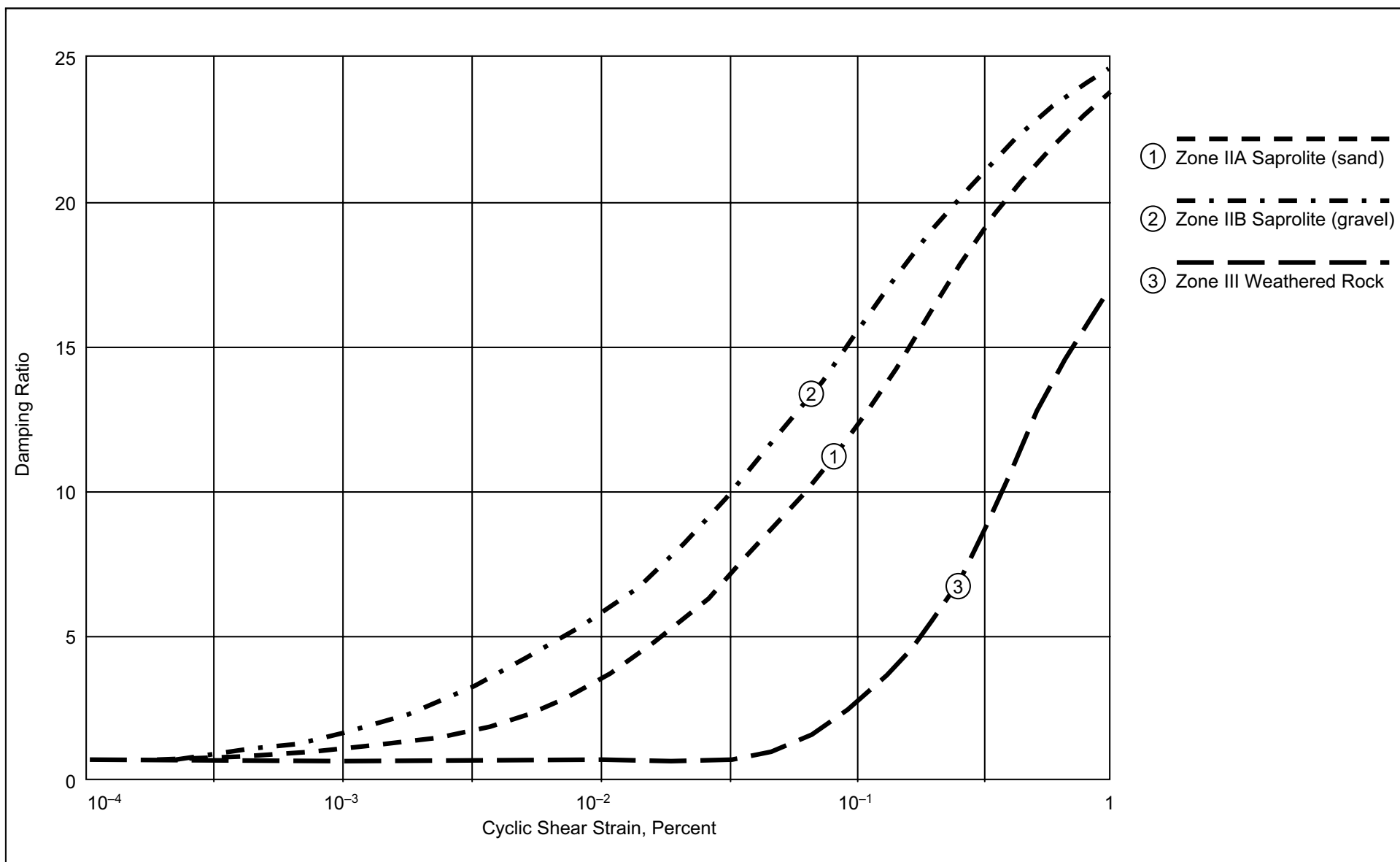


Figure 2.5-64 Variation of Damping Ratio with Cyclic Shear Strain

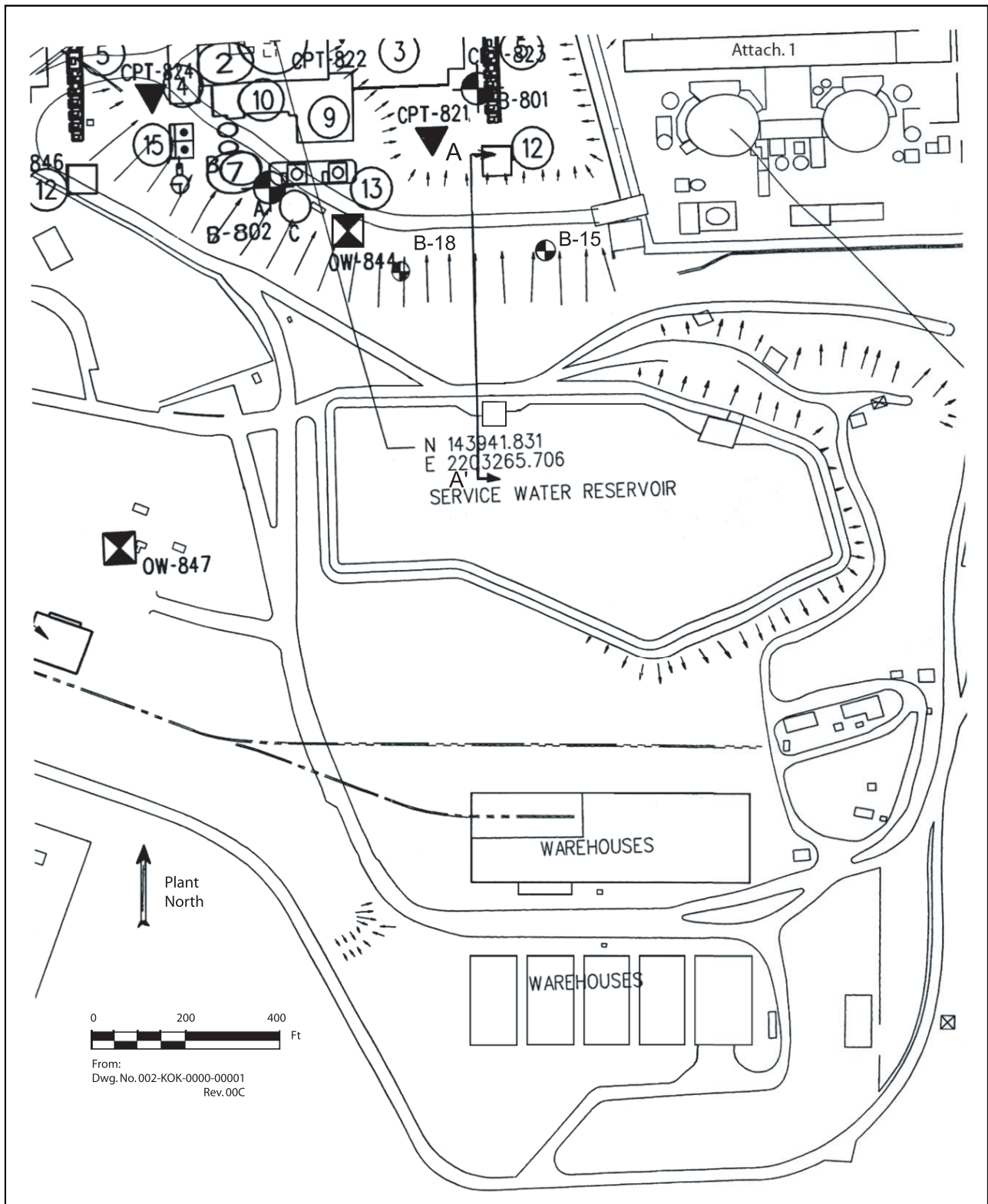


Figure 2.5-65 Plan View of Slope North of the SWR

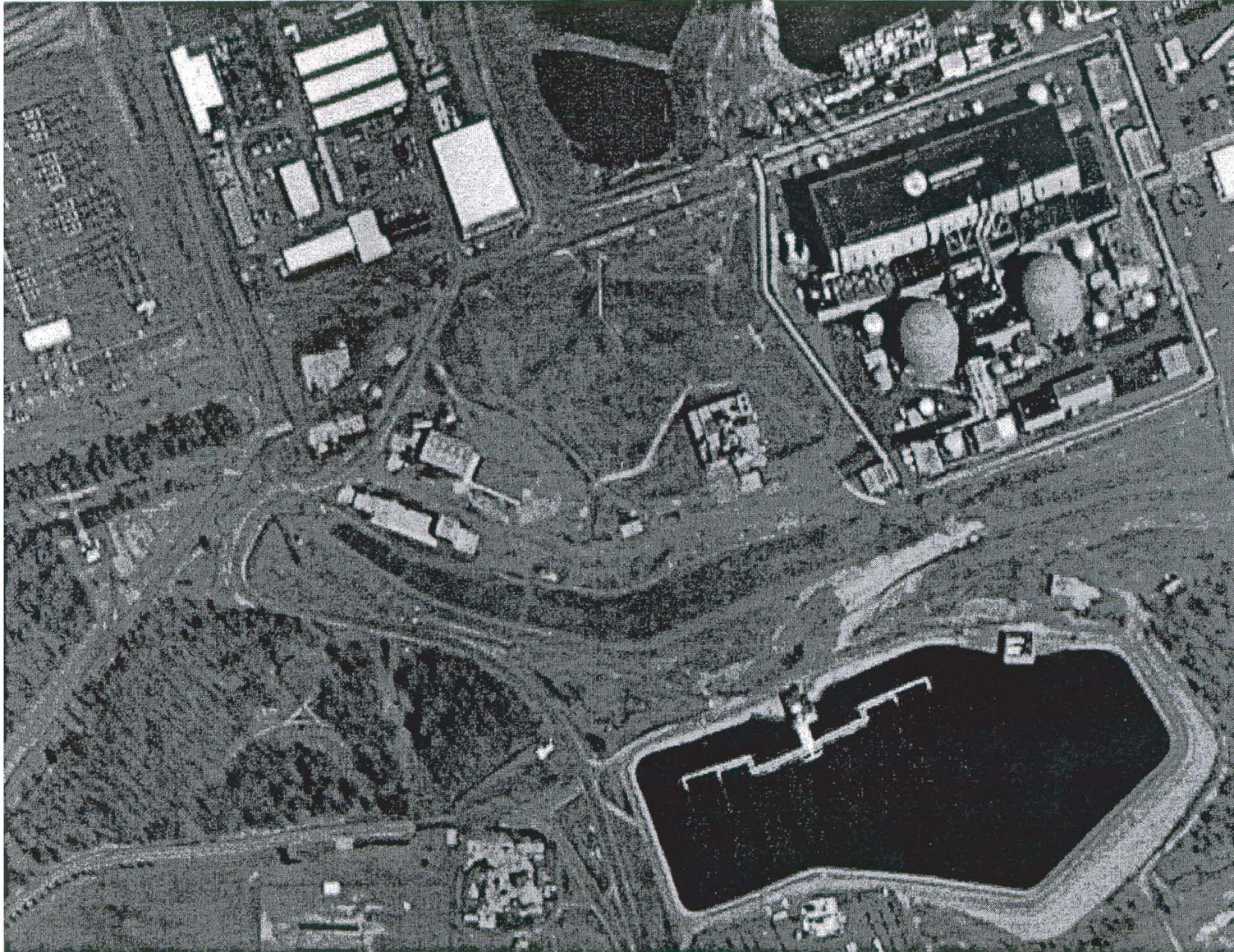


Figure 2.5-66 Photograph of Plan View of Slope North of the SWR



Figure 2.5-67 Photograph of Slope North of the SWR

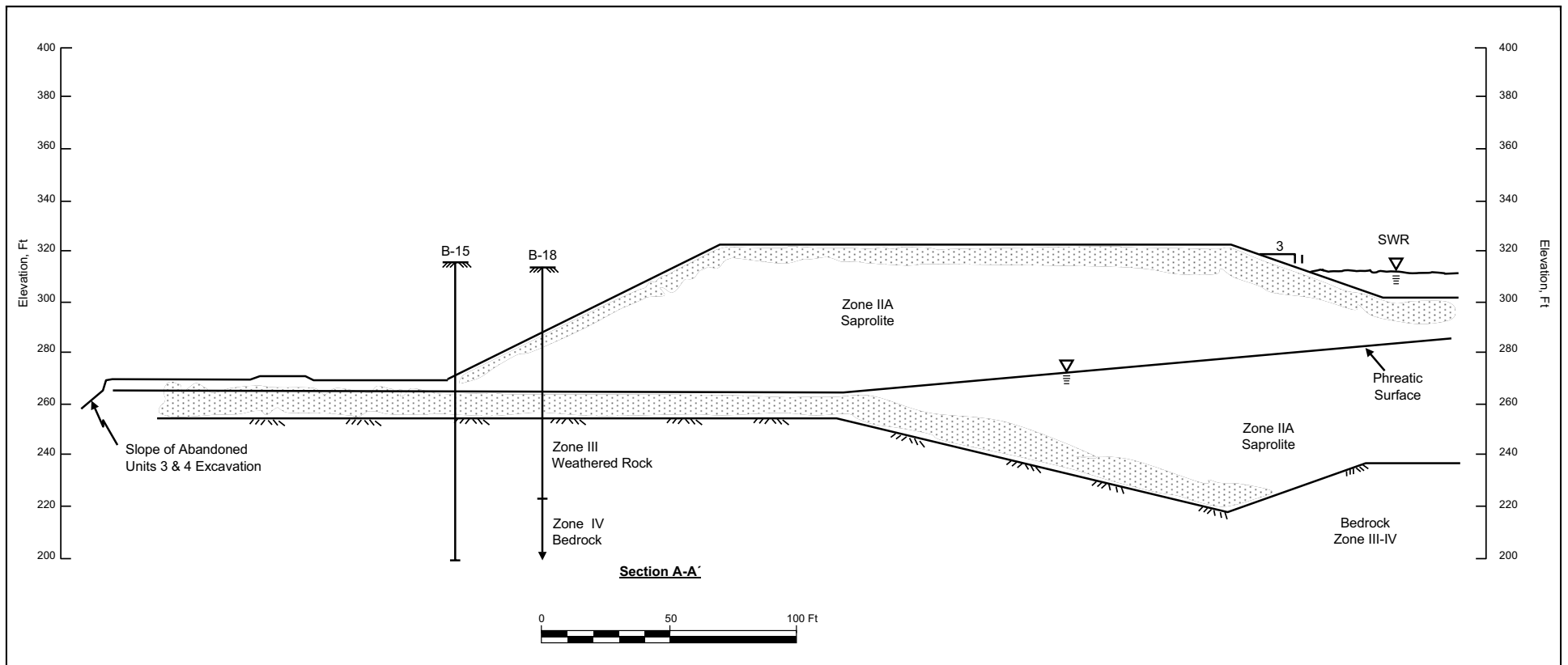


Figure 2.5-68 Cross-Section of Existing Slope North of the SWR

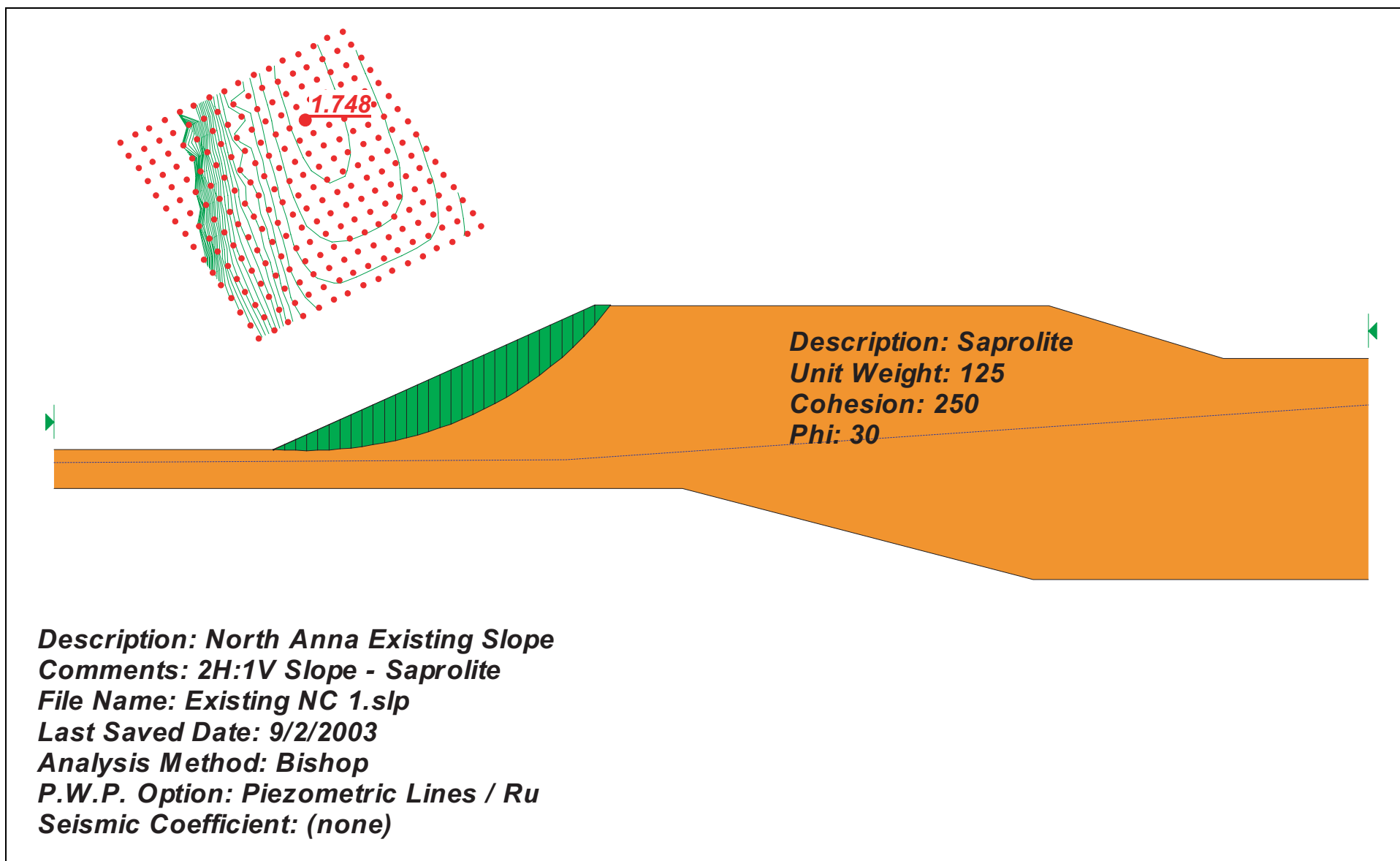


Figure 2.5-69 SLOPE/W Analysis of Long-Term Static Case

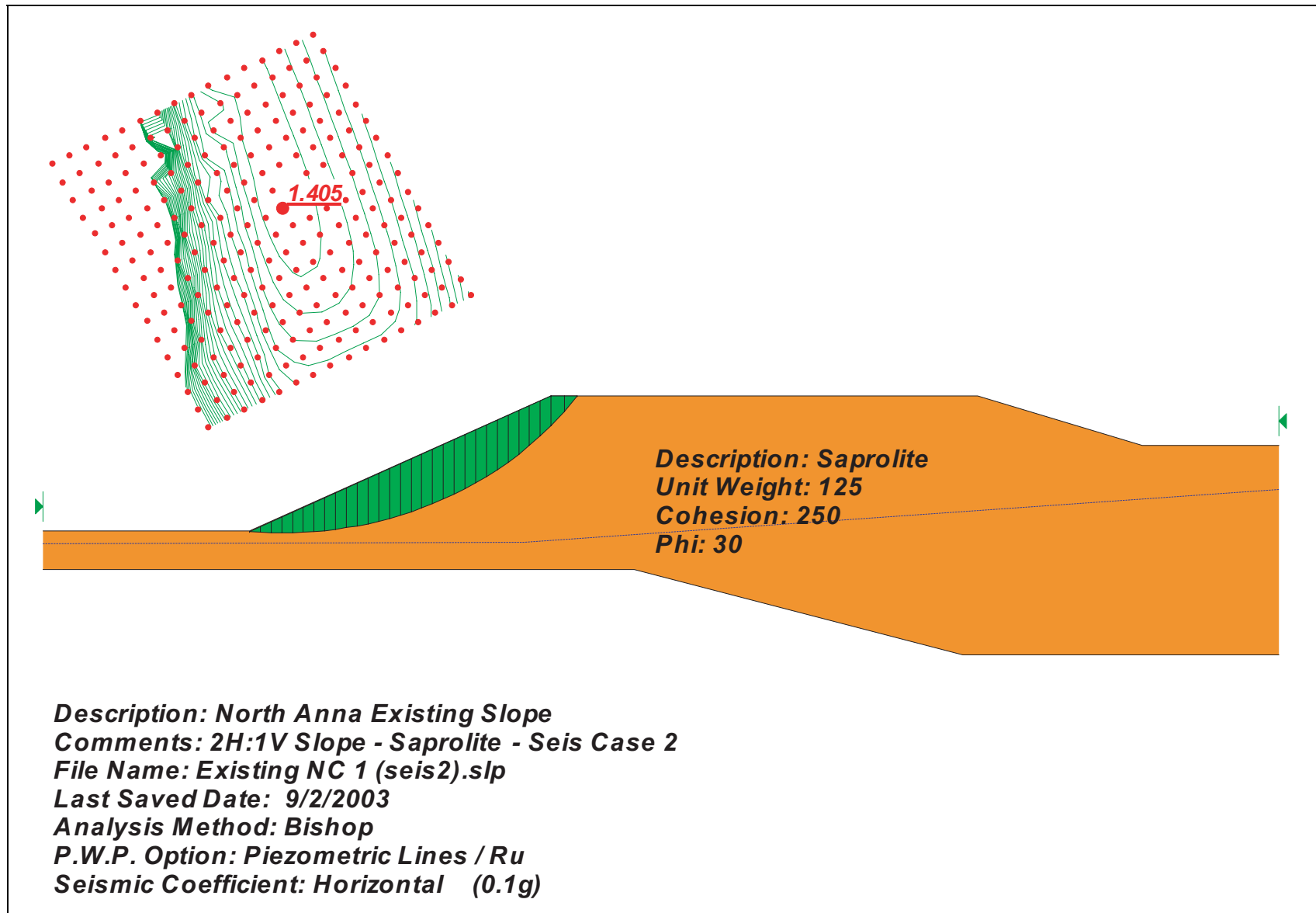


Figure 2.5-70 SLOPE/W Analysis of Seismic Case

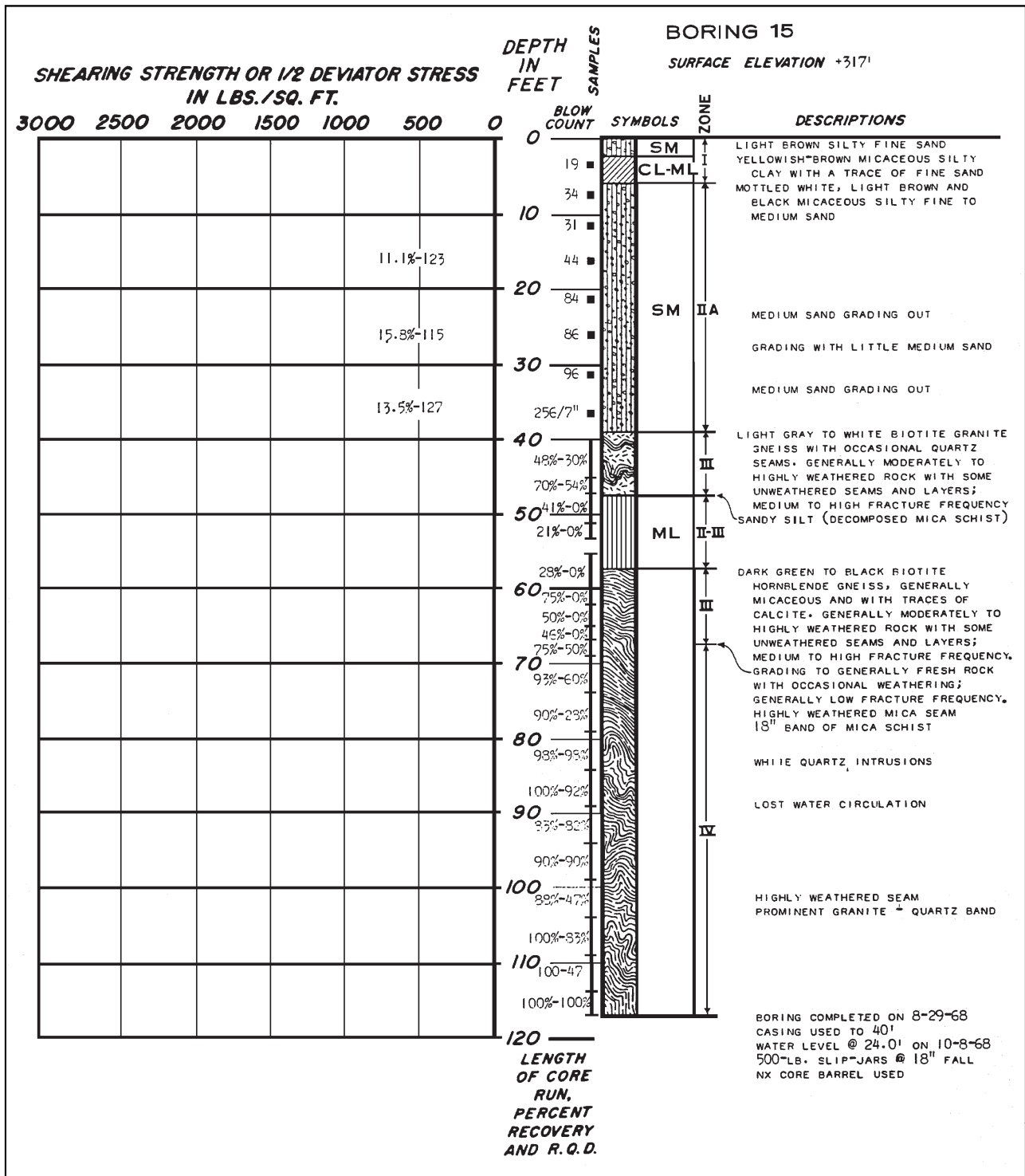


Figure 2.5-71 Log of Boring B-15

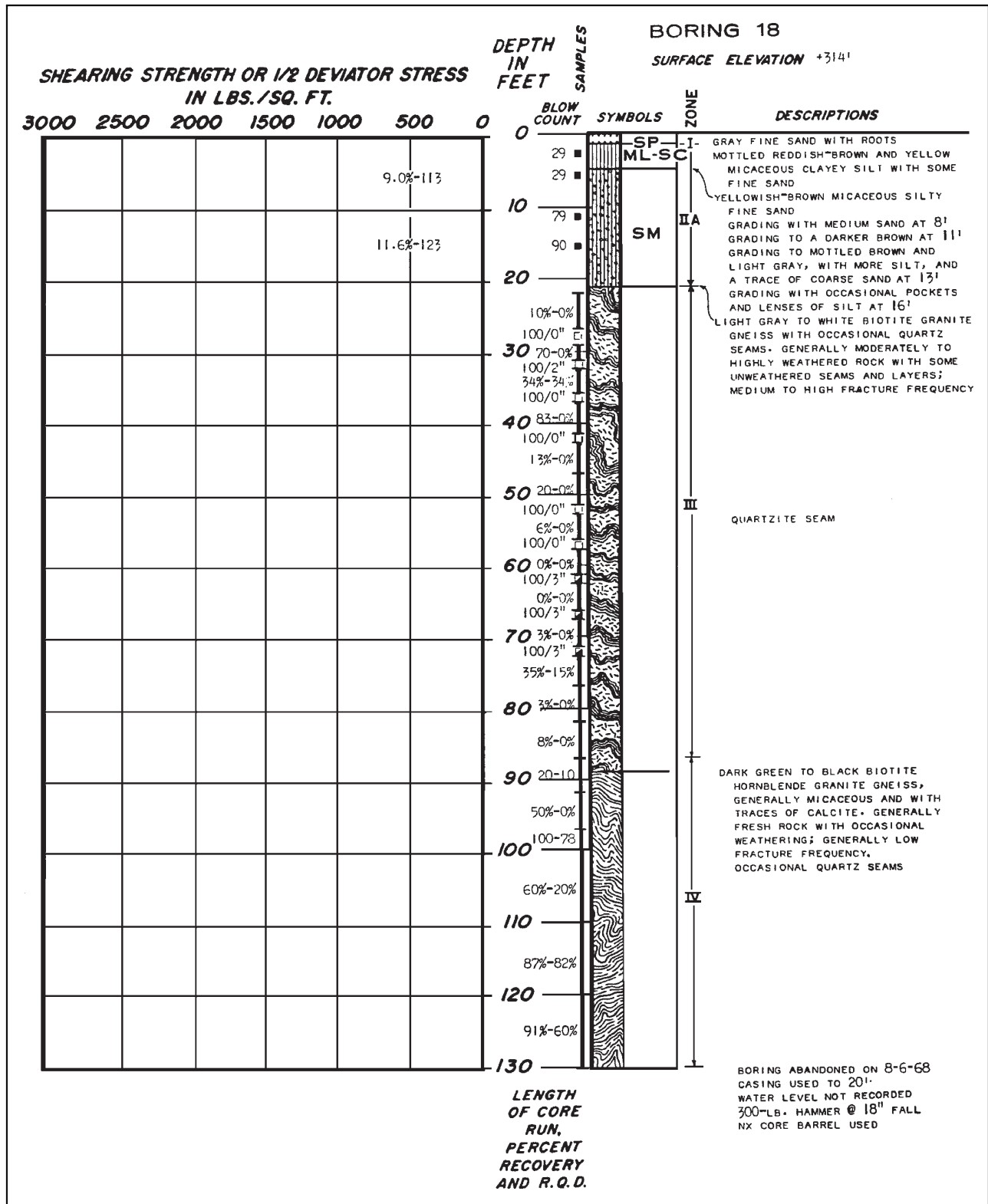


Figure 2.5-72 Log of Boring B-18